Catalysis Today xxx (2015) xxx–xxx

Contents lists available at ScienceDirect

Catalysis Today

journal homepage: www.elsevier.com/locate/cattod

Catalyst synthesis by continuous coprecipitation under micro-fluidic conditions: Application to the preparation of catalysts for methanol synthesis from CO_2/H_2

Laetitia Angelo[a], Maria Girleanu[b], Ovidiu Ersen[b], Christophe Serra[c], Ksenia Parkhomenko[a], Anne-Cécile Roger[a,*]

[a] *ICPEES, Équipe "Énergie et Carburants pour un Environnement Durable" UMR CNRS 7515, ECPM, Université de Strasbourg (UdS), 25 rue Becquerel, 67087 Strasbourg Cedex 2, France*
[b] *Institut de Physique et Chimie des Matériaux de Strasbourg (IPCMS), UMR 7504 CNRS-Université de Strasbourg (UdS), 23, rue du Loess, 67037 Strasbourg Cedex 2, France*
[c] *Université de Strasbourg (UdS), Ecole de Chimie Polymères et Matériaux (ECPM), Charles Sadron Institute (ICS) – UPR 22 CNRS, Precision Macromolecular Chemistry Group (CMP), 23 rue du Loess, BP84047, 67034 Strasbourg Cedex 2, France*

ARTICLE INFO

Article history:
Received 30 June 2015
Received in revised form 28 August 2015
Accepted 28 September 2015
Available online xxx

Keywords:
CO_2 hydrogenation
Methanol synthesis
CuO-ZnO-ZrO_2
Synthesis effect
Continuous coprecipitation

ABSTRACT

A new method of synthesis based on micro-fluidic continuous coprecipitation has been used to prepare CuO-ZnO-ZrO_2 catalyst. The catalytic behavior was then investigated for CO_2 hydrogenation into methanol and compared with a CuO-ZnO-ZrO_2 catalyst prepared by classical coprecipitation and with the same amount of Cu^0 (30%). The novel synthesis method allows a better repeatability and homogeneity of the catalyst which leads to the best methanol productivity of 486 g_{MeOH} kg_{cata}^{-1} h^{-1} at 280 °C under 50 bar and a GHSV of 10,000 h^{-1}.

1. Introduction

Numerous measures to reduce anthropogenic greenhouse gas emissions, especially CO_2, already exist such as its capture and storage. Another solution is to develop a method for converting CO_2 into valuable chemical compounds such as methanol, methane, formic acid or dimethylether [1–4]. The context of this work is to transform CO_2 emitted by industries into methanol by reduction with hydrogen produced by water electrolysis, using excess of electricity provided by decarbonized energies such as nuclear and renewable energies (Power to Liquid process). Beyond the valorization of CO_2, this process also allows to provide a management function for the electric grid. In fact, the production of hydrogen is correlated with the quantity of surplus electricity from the network.

Methanol is produced over 50 million tons per year [5] and is present in many industrial sectors. It is used as a raw material for the synthesis of formaldehyde, one of the most important organic molecules [6], for the synthesis of olefins [7,8] such as propylene and ethylene (biopolymer precursors). Methanol is also known as fuel [7,9–11] either for fuel cells [12,13] or mixed with gasoline, or indirectly as a raw material for the synthesis of diesel, gasoline, dimethylether, hydrocarbons. ... Thus the synthesis of methanol allows getting stable and easily stored carbon energy, as an alternative to fossil fuels.

At first methanol was mostly produced by catalytic hydrogenation of CO [14] with a feed gas of CO/H_2 or $CO/CO_2/H_2$. In the 90s some studies comparing the reactivity of CO/H_2 and CO_2/H_2 have shown that hydrogenation of CO_2 is faster than that of CO [15–17]. The same studies show that even starting from $CO/CO_2/H_2$ mixtures, methanol is mainly produced from hydrogenation of CO_2. Thereafter, in the early 2000s the number of publications about CO_2 hydrogenation increased.

The conventional methanol synthesis catalysts were designed for $CO/CO_2/H_2$ and must be optimized and modified for the hydrogenation of CO_2 without CO addition. The literature review clearly shows that copper is the favored metal and highlights the importance of the presence of ZnO along with a good interface between Cu and ZnO [18,19] for this reaction which increases respectively

* Corresponding author. Tel.: +33 (0)3 68 85 27 69; fax: +33 (0)3 68 85 27 68.
E-mail address: annececile.roger@unistra.fr (A.-C. Roger).

http://dx.doi.org/10.1016/j.cattod.2015.09.028
0920-5861/

the copper dispersion and the adsorption of CO_2. The beneficial effect of the support was also discussed for Cu/ZnO based catalysts. The addition of ZrO_2 leads to an increase of the copper dispersion and ZrO_2 is involved in the adsorption of CO_2 [20,21]. This higher metal dispersion is due to a large interfacial area of CuO and ZrO_2 favored by the formation of surface oxygen vacancies on the ZrO_2 support [22]. This high interfacial area was as well discussed to play a role in the improvement of the methanol formation due to microcrystalline copper particles which are stabilized by interaction with an amorphous zirconia support [23]. This is why it is important to have a right control of the synthesis parameters such as pH and temperature. These CuO-ZnO-ZrO_2 catalysts were synthesized by coprecipitation [24], a classical synthesis in discontinuous mode (batch) using a buffer solution of controlled pH [25] where nitrates are added in continuous and where the precipitating agent is used to regulate the pH throughout the reaction [26,27].

In this work we present the study of a new method of synthesis based on continuous coprecipitation to overcome the problems of repeatability and homogeneity of solutions and conditions during the conventional coprecipitation. It was inspired by the use of the micromixer [28,29] or microemulsion [30]. This continuous method is based on the formation of droplets formed by reagents brought about an immiscible fluid carrier [31]. These droplets are more precisely formed by the merger of two droplets, each containing one of the starting aqueous solutions [32,33]. Upon the merger of these solutions, coprecipitation occurs, allowing the same environment and the same conditions (pH and temperature) for each droplet during the coprecipitation, leading to better repeatability and homogeneity.

Here are presented the effects of the catalyst synthesis conditions on the characterization and the catalytic behavior of efficient CuO-ZnO-ZrO_2 catalysts in CO_2 hydrogenation into methanol.

2. Experimental

2.1. Catalyst preparation

Two CuO-ZnO-ZrO_2 catalysts were synthesized by two different coprecipitation methods: a coprecipitation at constant pH and a continuous coprecipitation. These catalysts contain 37.5% by weight of CuO (corresponding to 30% Cu^0), 41 wt% of ZnO and 21.5 wt% of ZrO_2. The notation is exemplified as follows: 30CuZn-Z_X refers to a catalyst containing 30 wt% of Cu^0 completed by zinc oxide and zirconia where X corresponds to the synthesis method (pH = coprecipitation at constant pH and M = micro-fluidic continuous coprecipitation).

The constant pH coprecipitation [34,35] was realized in a buffer solution at pH 6–6.5 heated at 60–65 °C. A solution (1 M) of Cu nitrate, Zn nitrate and ZrO nitrate was added drop by drop in parallel with a solution of Na_2CO_3 (1.6 M), used as precipitating agent and pH control leading to a 1.13 molar ratio of carbonate/metal cations. The precipitate was aged for 3.5 h in the mother liquor, and then filtered, washed with water and dried for 5 days at 100 °C.

The micro-fluidic continuous coprecipitation was realized in a micro-fluidic system (Scheme 1) [36] by a continuous formation of little droplets, of diameter around 1 mm, made by the solution of nitrates (1 M) and the precipitating agent (1.6 M Na_2CO_3) in a constant flux (0.9 mL min^{-1}) of silicon oil. The aqueous solutions are delivered to a constant total flow of 40 μL min^{-1} with a 1.13 molar ratio of carbonate/metal cations. The precipitate was aged for one night in the mother liquor, and then the aqueous phase is separated, filtered, washed with water and dried for 2 days at 100 °C.

The resulting powders were then calcined in air at 400 °C for 4 h with a heating ramp of 2 °C min^{-1} to give fresh catalysts.

2.2. Catalyst characterization

The catalyst apparent density was determined using a cylindrical glass tube of internal diameter of 1.5 cm, on fresh catalyst initially sieved to particle size fraction between 100 and 125 μm.

Specific surface areas measurements were performed by nitrogen adsorption–desorption at −196 °C using the Brunauer-Emmet-Teller (BET) method on a Micromeritics ASAP 2420 apparatus. Samples were previously outgassed at 250 °C for 3 h to remove the adsorbed moisture.

The crystalline structure of the catalysts was determined by X-ray diffraction (XRD) with a Bruker D8 Advance diffractometer equipped with a LYNXEYE detector and a Ni filter for Cu Kα radiations over a 2θ range of 10–95° and a step of 0.016° every 0.5 s. The crystallite size was calculated using the Debye-Scherrer equation [37].

Reducibility studies were performed by temperature programmed reduction (TPR) on a Micromeritics AutoChem II 2920 with 400 mg of fresh catalyst and a total gas flow rate of 50 mL min^{-1} of 10% H_2 in Ar with a heating ramp of 1 °C min^{-1} until 300 °C.

Metal surface area was determined by N_2O reactive frontal chromatography [38,39] on a Micromeritics AutoChem II 2920 in 50 mL min^{-1} of 2% N_2O in Ar. Approximately 400 mg of fresh catalyst were first reduced at 300 °C for 12 h under a flow of 50 mL min^{-1} of 10% H_2 in Ar and then cooled to 50 °C after a Ar purge. The copper surface area was calculated by quantifying the amount of consumed N_2O and assuming 1.46×10^{19} copper atoms per square meter [40].

The morphology after calcination was studied using conventional transmission electron microscopy (TEM) as well as scanning transmission electron microscopy (STEM) or electron tomography. All the investigations were performed on a JEOL 2100F TEM/STEM microscope, operating at 200 kV and equipped with a probe corrector and a GIF Tridiem energy filter. For S/STEM analyses, after sonication of the catalysts powder in ethanol, a droplet of the solution was dropped on a holy carbon silver TEM grid.

For the electron tomography analysis, a high tilt sample holder from GATAN Company was used in order to acquire the tilt image series. The angles range from +65 to −65 degrees, with projections taken every 2° according to Saxton scheme. 84 TEM images were recorded per tilt series with a cooled GATAN ULTRASCAN 1000 CCD

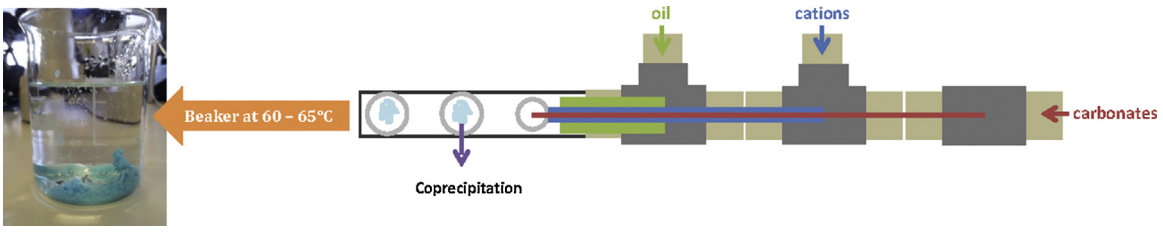

Scheme 1. Schematization of micro-fluidic continuous coprecipitation.

Please cite this article in press as: L. Angelo, et al., Catalyst synthesis by continuous coprecipitation under micro-fluidic conditions: Application to the preparation of catalysts for methanol synthesis from CO_2/H_2, Catal. Today (2015), http://dx.doi.org/10.1016/j.cattod.2015.09.028

detector (2048 × 2048 pixels with a pixel size of 0.2 nm). The images were first roughly aligned using a cross-correlation algorithm. A refinement of this initial alignment and a precise determination of the tilt axis direction were then obtained using the IMOD software where the centers 5 nm Au NPs were used as fiducial markers [41]. The volume reconstructions have been computed using an iterative approach consisting of a simultaneous algebraic reconstruction technique implemented using the TOMO3D software. [42] The number of iterations did not exceed 30. Visualization of the final volumes was carried out using ImageJ software.

For the high angle annular dark field STEM (HAADF-STEM) analyses the camera focal length used in HAADF was 10 cm, corresponding to inner and outer diameters of the annular detector of 60 mrad and 160 mrad, respectively. Furthermore, the limit resolution in HAADF-STEM mode was about 0.11 nm. Moreover, EDX analyses in HAADF-STEM mode were performed on various fragments of 30CuZn-Z samples. The exposure time and the spectra were been performed using the DigiScan routine for Digital Micrograph software.

2.3. Catalytic activity

The carbon dioxide hydrogenation into methanol was performed in a stainless steel fixed bed reactor with an internal diameter of 1 cm. The powdered catalyst was initially sieved to particle size fraction between 100 and 125 μm to obtain a bed volume of 0.24 cm^3. The reaction temperature was controlled by a thermocouple located in the furnace and contacting the external metallic walls of the reactor at the level of the catalytic bed. The gas flows were regulated by mass flow controllers in order to deliver a constant total flow rate of 40 mL min^{-1} of $H_2/CO_2/N_2$.

The catalyst was first reduced under H_2 (6.18 mL min^{-1}) at 300 °C and 50 bar for 12 h with a ramp of 1 °C min^{-1}. After cooling the catalyst to 100 °C, the gas flows were adjusted to deliver the reaction flow of 35 mL min^{-1} of H_2:CO_2 (3.89:1) and 5 mL min^{-1} of N_2 (as internal standard). After the purge, the temperature is first increased to 150 °C to analyze the compounds of the gas phase before the reaction. The CO_2 hydrogenation was then carried out at different temperatures between 240 and 320 °C under 50 bar and a Gas Hourly Space Velocity (GHSV) of 10,000 h^{-1}.

The analysis of the reaction products was performed in two steps. First the outgas was analyzed online every 30 min using a gas microchromatograph (Inficon 3000 Micro GC) equipped with a TCD detector and two columns: a PoraPlot Q column to separate N_2, CO, CH_4, CO_2, CH_3OH and a molecular sieve 5 Å column to separate N_2, H_2, CH_4, CO. Secondly, the liquid phase collected in the trap during the reaction was recovered at the end of the reaction and then analyzed offline using a gas chromatograph (Agilent Technologies 6890N Network GC Systems) with ZB-WAX Plus (Zebron) column to quantify methanol.

The conversions (X_{CO_2} and X_{H_2}) and selectivities (S_{CH_3OH} and S_{CO}) were then determined by the total carbon balance of the gas phase and the liquid phase. The methanol productivity was calculated in the same way by two methods: one giving productivity per catalyst mass ($g_{MeOH}\ kg_{cata}^{-1}\ h^{-1}$) and the other one giving productivity per copper surface area ($mg_{MeOH}\ m^{-2}{}_{Cu}\ h^{-1}$).

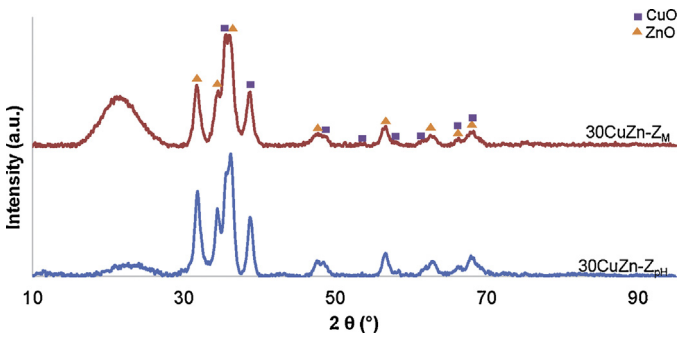

Fig. 1. XRD of the fresh 30CuZn-Z_{pH} and 30CuZn-Z_M catalysts.

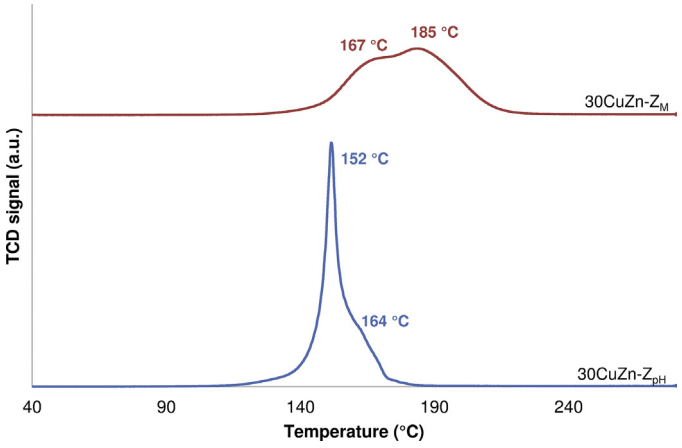

Fig. 2. TPR profiles of the fresh 30CuZn-Z_{pH} and 30CuZn-Z_M catalysts.

3. Results and discussion

3.1. Characterization

The main characteristics of the fresh CuO-ZnO-ZrO_2 catalysts are given in Table 1. The apparent density of the catalyst prepared by coprecipitation at constant pH is higher than that of catalyst synthesized by continuous coprecipitation, 0.51 compared to 0.35 g cm^{-3}, respectively.

The specific surface areas changes from 79 $m^2\ g^{-1}$ to 40 $m^2\ g^{-1}$ for 30CuZn-Z_{pH} and 30CuZn-Z_M, respectively. The highest BET surface is then observed for the catalyst prepared by coprecipitation at constant pH. However no correlation was found between BET surfaces and pore characteristics. The mean pore volume diameter of

Table 1
Characterizations of the fresh 30CuZn-Z_{pH} and 30CuZn-Z_M catalysts.

Catalyst	Apparent density (g cm^{-3})	BET			XRD-Crystallite size (nm)		Cu surface area[d] ($m^2\ g_{cata}^{-1}$)
		S_{BET}[a] ($m^2\ g^{-1}$)	D_{pore}[b] (nm)	V_{pore}[c] ($cm^3\ g^{-1}$)	CuO	ZnO	
30CuZn-Z_{pH}	0.51	79	17	0.38	10.0	10.4	10.5
30CuZn-Z_M	0.35	40	20	0.37	9.7	8.8	14.5

[a] Specific surface area.
[b] Pore diameter.
[c] Pore volume.
[d] Determined by N_2O chemisorption.

Please cite this article in press as: L. Angelo, et al., Catalyst synthesis by continuous coprecipitation under microfluidic conditions: Application to the preparation of catalysts for methanol synthesis from CO_2/H_2, Catal. Today (2015), http://dx.doi.org/10.1016/j.cattod.2015.09.028

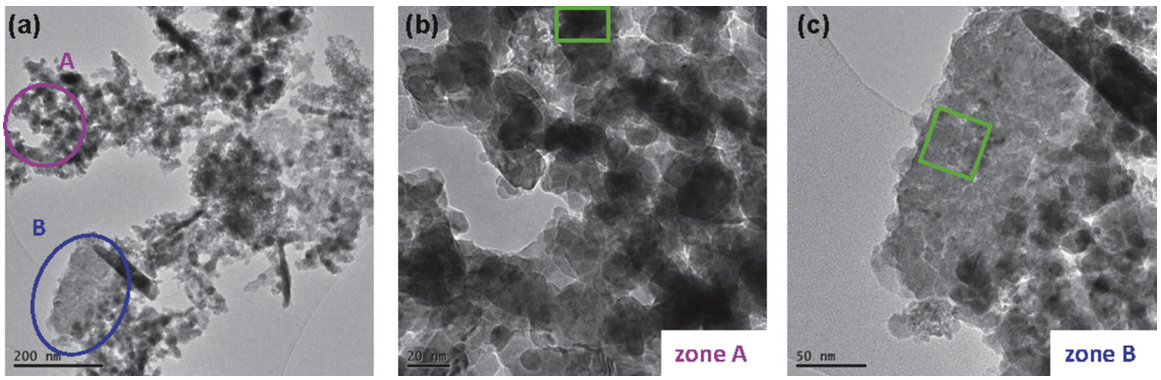

Fig. 3. Bright field TEM images of 30CuZn-Z_{pH} catalyst: (a) representative fragment highlighting the two types of morphologies, (b) zone A (large particles) and (c) zone B (small particles).

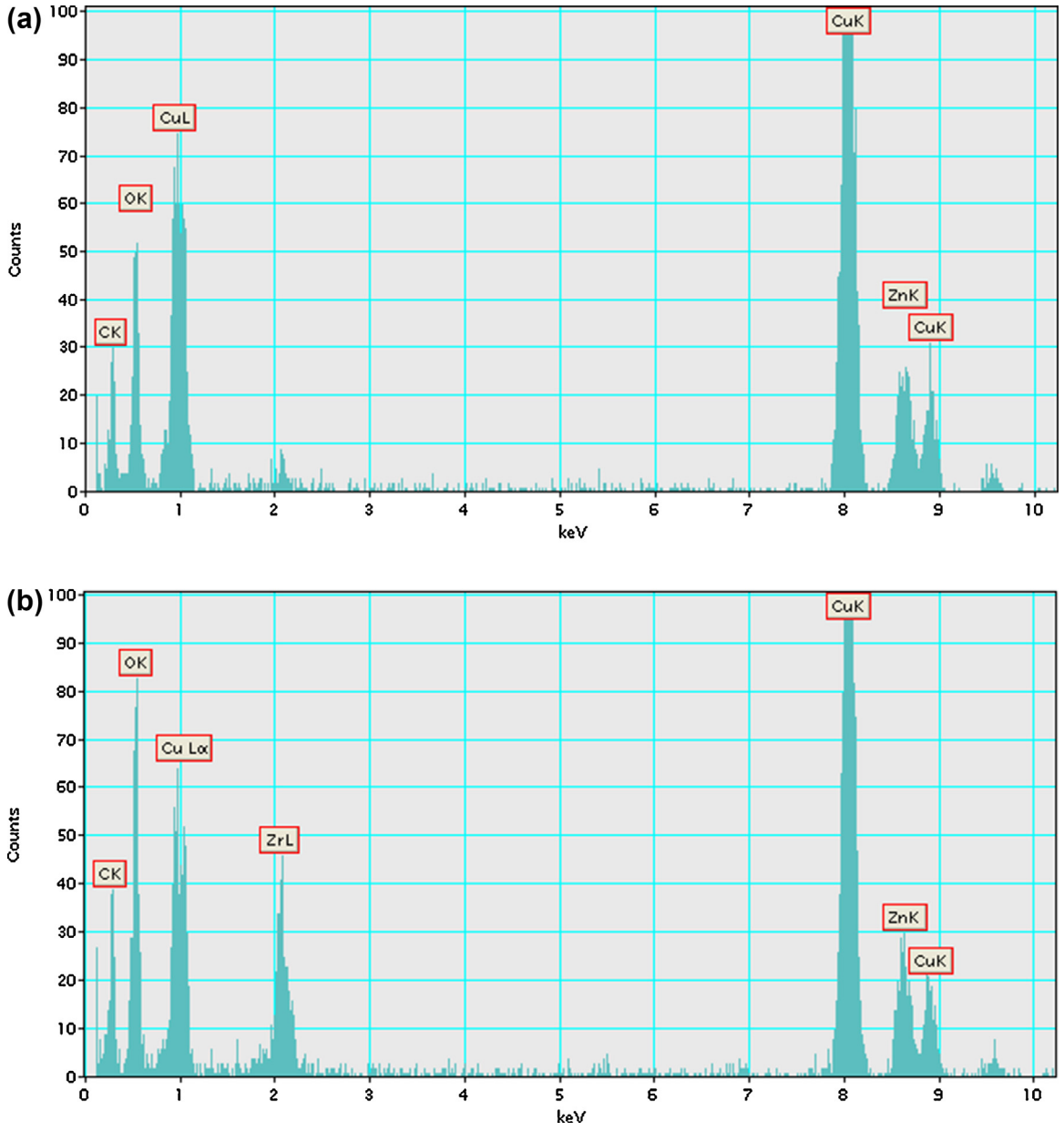

Fig. 4. EDX analysis of the 30CuZn-Z_{pH} catalyst corresponding to (a) zone A (large particles) and (b) zone B (small particles).

Please cite this article in press as: L. Angelo, et al., Catalyst synthesis by continuous coprecipitation under microfluidic conditions: Application to the preparation of catalysts for methanol synthesis from CO_2/H_2, Catal. Today (2015), http://dx.doi.org/10.1016/j.cattod.2015.09.028

these catalysts is around 20 nm independently of the preparation method, and in spite of different specific surface areas, same pore volumes were calculated (around 0.38 $cm^3\ g^{-1}$).

The crystalline structures of the catalysts after calcination are presented in Fig. 1. Diffraction peaks corresponding to copper oxide and zinc oxide are observed for both catalysts. The zirconium oxide diffraction peaks are not observed suggesting that this phase is in an amorphous or a micro-crystallite state [43]. The wide peak located between a 2θ of 15° and 30° is due to the sample holder glass. By comparing both methods of synthesis, same diffractograms are obtained and also similar CuO and ZnO crystallite sizes, around 10 nm (Table 1), supposing that the choice of the synthesis does not lead to deep modifications in catalyst structure.

The reducibility of copper species was determined by TPR experiments and the results are presented in Fig. 2. For 30CuZn-Z_{pH}, TPR profile shows one reduction peak at 152 °C with a shouldered peak at 164 °C suggesting two reduction steps, probably because of different insertions or interactions between copper and the support [38]. This profile can be explained by distinct copper oxide reduction steps, the first one related to the reduction of small crystalline CuO clusters, and the second one attributed to a strong interaction between copper ions and the support [38]. The use of microfluidic continuous coprecipitation to prepare 30CuZn-Z_M catalyst modifies the reduction profile leading to two reduction peaks but which are spread over a wide zone (between 140 °C and 210 °C) and are switched to higher temperatures (peaks at 167 °C and 185 °C).This suggests that the micro-fluidic preparation method leads to a modification of CuO-support interactions. The theoretical hydrogen consumption (4.72 $mmol_{H_2}\ g^{-1}$) was compared to the values obtained for 30CuZn-Z catalysts and the reduction percentage of CuO to Cu^0 were determined assuming the only reduction of CuO and a copper oxide content of 30% (respectively 98% and 105% for 30CuZn-Z_{pH} and 30CuZn-Z_M). The catalysts present finally similar reducibility closed to 100% confirming a total copper reduction.

The copper surface areas calculated by N_2O reactive frontal chromatography are given in Table 1. The highest copper surface area is observed for 30CuZn-Z_M (14.5 $m^2\ g_{cata}^{-1}$) which presented the lowest BET surface area and not for 30CuZn-Z_{pH} (10.5 $m^2\ g_{cata}^{-1}$) whose BET surface area was of 79 $m^2\ g_{cata}^{-1}$, suggesting that a high copper surface area is not directly correlated with a high BET surface.

The catalyst morphology after calcination observed by TEM is shown in Fig. 3 for 30CuZn-Z_{pH}. This catalyst presents two different morphologies: a first region (zone A) composed of large particles and a second region (zone B) composed of small particles. This highlights an inhomogeneous morphology of the sample. To better understand this inhomogeneity, STEM-EDX analyses (Fig. 4) in these two regions were conducted. It shows that the zone A is rich in zinc with a high level of copper but only a few traces of zirconium, while for the zone B a high level of both zirconium and copper is observed. The same observations were made by analyzing different areas of the sample. The copper oxide is then present in both regions. In order to have a better understanding of the copper oxide dispersion in these two regions, electron tomography approach was used. It provides a three dimensional representation of the studied object and the location of different phases within the material. The reconstruction volume of a representative fragment of 30CuZn-Z_{pH} catalyst is presented in Fig. 5. The zone A, rich in zinc oxide, shows that copper covers part of the surface of large ZnO particles, evidenced by red arrows in Fig. 5. In contrary, in the zone B, rich in zirconium oxide, copper oxide is under the form of nanoparticles (green arrows) dispersed on ZrO_2. The CuO particle sizes were different depending on the zone: zone A ≈ 5.5 nm and zone B ≈ 2.4 nm. These results evidence a different distribution of copper oxide depending on the region nature.

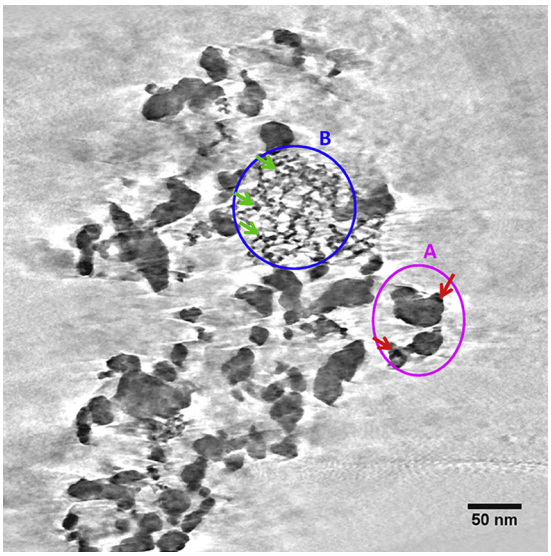

Fig. 5. Section in the reconstructed volume of a representative fragment of the 30CuZn-Z_{pH} catalyst.

Similar study has been performed on 30CuZn-Z_M catalyst and the results are presented in Figs. 6–9. This catalyst does not present two regions contrary to 30CuZn-Z_{pH} and seems to be more homogeneous (Fig. 6 compared to Fig. 3). In fact, the three oxides (CuO, ZnO and ZrO_2) location is clearly less obvious to distinguish than for 30CuZn-Z_{pH}. Furthermore, the EDX analysis of the zone 1 of Fig. 6a detailed in Fig. 7 and Fig. 8, shows the presence of copper, zinc and zirconium regardless to the area studied. The presence of silver on the EDX analysis is due to the use of a silver grid. These results attest for a better homogeneity of the catalyst 30CuZn-Z_M prepared by continuous coprecipitation. The electron tomography analysis (Fig. 9) highlights the presence of two CuO particles sizes: around 5.3 nm (pink circle) and 2 nm (red arrow), corresponding respectively to the previously observed sizes for the two zones, one rich in zinc and the second rich in zirconium, for 30CuZn-Z_{pH}. Consequently, there seems to be the presence of two different morphologies but which are not obvious to distinguish. It is thus difficult to conclude if the zinc oxide and the zirconia are mixed or if a ZnO layer covers a zirconia layer. However the assumed better homogeneity for 30CuZn-Z_M explains the highest copper surface area.

These results obtained by TEM analysis were also used to highlight the zirconium oxide state that could not be previously determined by XRD. Since no crystalline lattice has been observed on the particles attributed to zirconia, ZrO_2 is considered amorphous in the studied samples.

3.2. Catalytic activity

The results obtained for 30CuZn-Z catalysts in CO_2 hydrogenation reaction at 240, 260, 280, 300 and 320 °C at 50 bar and with a GHSV of 10,000 h^{-1} are presented in Table 2.

Firstly the influence of reaction temperature on catalytic activity was studied. The catalytic results indicate that the conversions of H_2 and CO_2 increase gradually with the reaction temperature until 280 °C when the H_2 conversions stabilize around 9% whereas the CO_2 conversions keep increasing from 22% at 280 °C to 26% to 320 °C. These results are directly correlated to a progressive decrease in methanol selectivity (at 240 °C,

Please cite this article in press as: L. Angelo, et al., Catalyst synthesis by continuous coprecipitation under microfluidic conditions: Application to the preparation of catalysts for methanol synthesis from CO_2/H_2, Catal. Today (2015), http://dx.doi.org/10.1016/j.cattod.2015.09.028

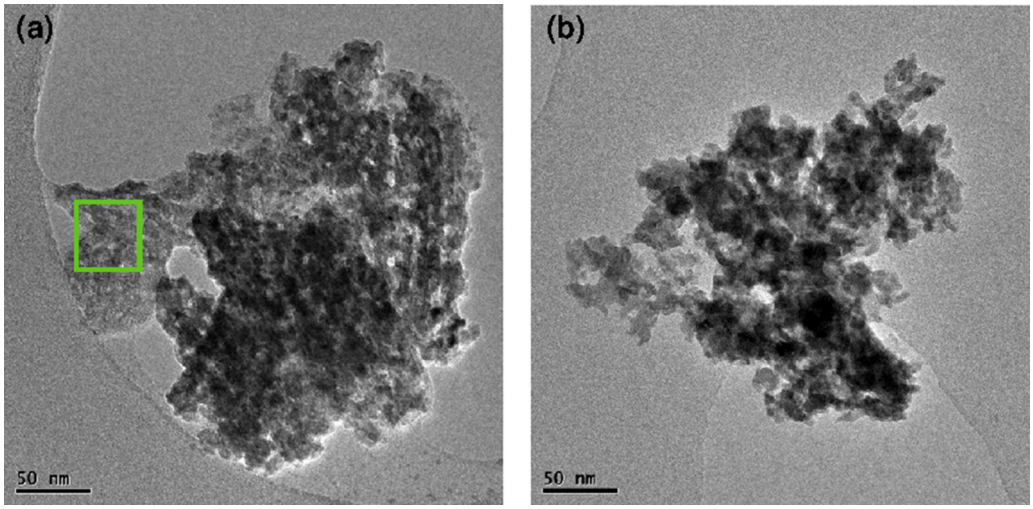

Fig. 6. Bright field TEM images of two areas of the catalyst 30CuZn-Z_M (a) area 1 and (b) area 2.

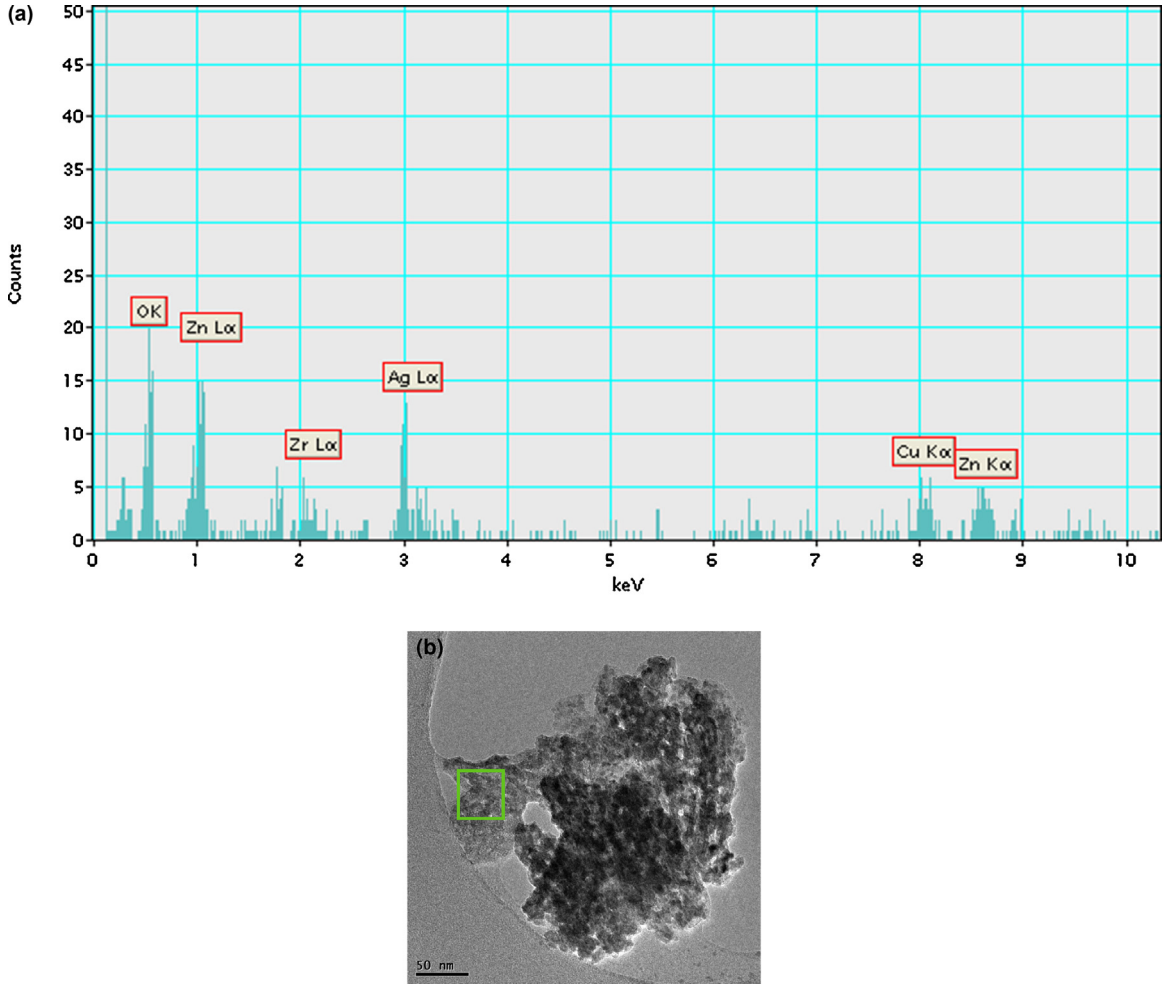

Fig. 7. (a) EDX analysis of the area 1 of the 30CuZn-Z_M catalyst in region 1 (b).

$S_{CH_3OH} \approx 50\%$ and at 320 °C, $S_{CH_3OH} \approx 14\%$) in favor of carbon monoxide selectivity (at 240 °C, $S_{CO} \approx 50\%$ and at 320 °C, $S_{CO} \approx 86\%$). The stabilization of H_2 conversion is directly related to these selectivity changes due to different H_2/CO_2 stoichiometry depending of these two competitive reactions. First the H_2/CO_2 stoichiometry is 3 (corresponding to the methanol synthesis produced by CO_2 hydrogenation), then with the temperature increase, this is the Reverse Water Gas Shift reaction with a H_2/CO_2 stoichiometry of 1 which is favored. No noticeable catalyst deactivation was observed over the tests.

Please cite this article in press as: L. Angelo, et al., Catalyst synthesis by continuous coprecipitation under microfluidic conditions: Application to the preparation of catalysts for methanol synthesis from CO_2/H_2, Catal. Today (2015), http://dx.doi.org/10.1016/j.cattod.2015.09.028

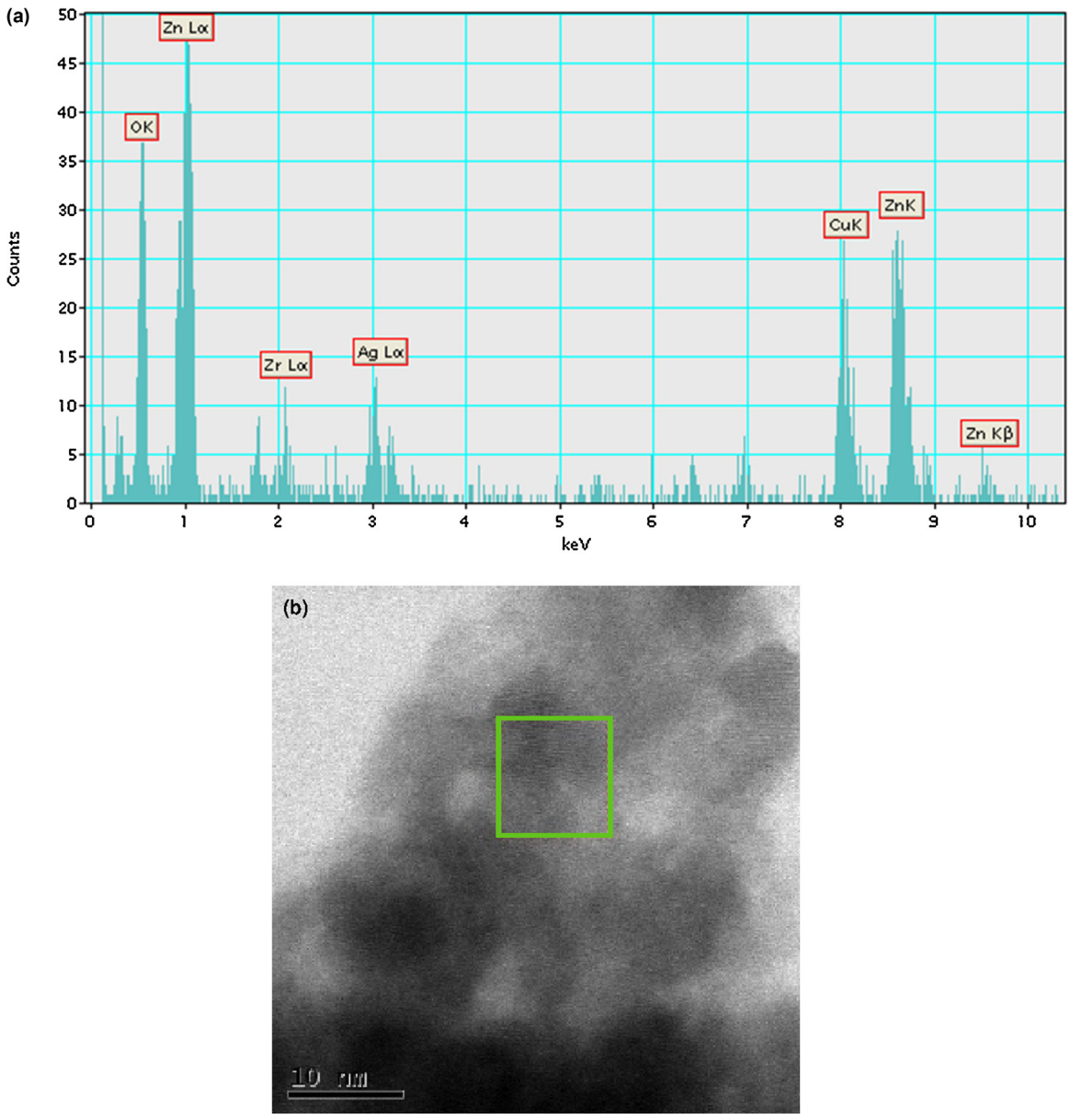

Fig. 8. (a) EDX analysis of the area 1 of the 30CuZn-Z_M catalyst in the region 2 (b).

Secondly the influence of synthesis method on catalytic activity was investigated by comparing the results of both catalyst for CO_2 hydrogenation. The conversions of 30CuZn-Z_M at 260 °C show identical values to those of 30CuZn-Z_{pH} at 240 °C: $H_{H_2} \approx 7\%$ and $X_{CO_2} \approx 14\%$. In this way, the 30CuZn-Z_M conversions correspond, at low temperature, to those of 30CuZn-Z_{pH} but for temperatures of 20 °C higher. However, this gap is not observed for selectivities which are similar at iso temperature, for example at 280 °C the methanol selectivity is of 34% for both catalysts. The 30CuZn-Z_M catalyst presents similar methanol productivities at low temperature and better methanol productivities at high temperature in comparison with 30CuZn-Z_{pH} catalyst. In order to have a better understanding of these results, the methanol productivities are presented at iso conversions of H_2 and CO_2 (Fig. 10). The 30CuZn-Z_M catalyst shows the best productivities per catalyst mass and similar productivities per copper surface area. These results can be explained by a lower apparent density (0.35) and a higher Cu^0 surface (14.5 $m^2_{Cu^0}\ g_{cata}^{-1}$) for this catalyst prepared by a microfluidic continuous coprecipitation. These two catalysts present finally similar intrinsic activity. However, the best methanol productivity is obtained for 30CuZn-Z_M at 280 °C with 486 $g_{MeOH}\ kg_{cata}^{-1}\ h^{-1}$.

In the literature similar catalysts were also studied. With a Cu-ZnO-ZrO_2 catalyst containing similar amount of metallic copper, Arena et al. [44] have obtained a CO_2 conversion of 16.4%, a methanol selectivity of 38% and a methanol productivity of 1 $mg_{MeOH}\ m^{-2}{}_{cata}\ h^{-1}$ at 240 °C, 30 bar, GHSV of 8800 $NL\ h^{-1}\ kg_{cata}^{-1}$ and $H_2/CO_2 = 3$. In another publication [45] by increasing the copper content from 30 to 60 wt%, better CO_2 conversions (18%) and methanol selectivity (51%) were obtained. The methanol productivity was also improved to 305 $g_{MeOH}\ kg_{cata}^{-1}\ h^{-1}$ at 240 °C, 30 bar, GHSV of 10,000 $NL\ h^{-1}\ kg_{cata}^{-1}$ and $H_2/CO_2 = 3$. By modifying some parameters like increasing the GHSV at 80,000 $NL\ h^{-1}\ kg_{cata}^{-1}$, a clearly higher methanol productivity of 1200 $g_{MeOH}\ kg_{cata}^{-1}\ h^{-1}$ was obtained. Saito et al. [46] have also published results from 50Cu-ZnO-ZrO_2 catalyst leading to 665 $g_{MeOH}\ kg_{cata}^{-1}\ h^{-1}$ of methanol productivity at 250 °C, 50 bar, GHSV of 10,000 $L\ h^{-1}$ and $H_2/CO_2 = 3$. Compared to these results, our catalyst appears very promising even if it still needs to be optimized.

Please cite this article in press as: L. Angelo, et al., Catalyst synthesis by continuous coprecipitation under microfluidic conditions: Application to the preparation of catalysts for methanol synthesis from CO_2/H_2, Catal. Today (2015), http://dx.doi.org/10.1016/j.cattod.2015.09.028

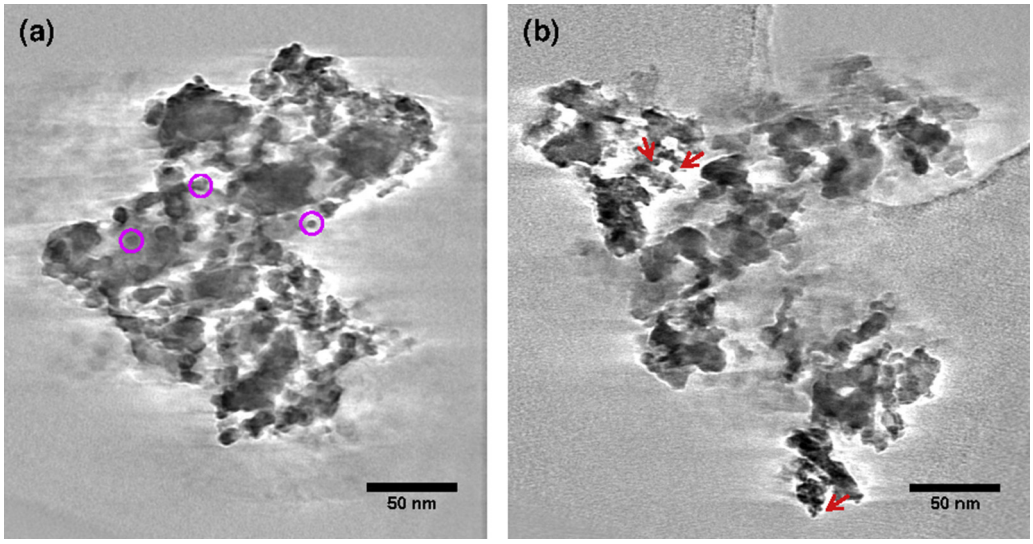

Fig. 9. Sections in the reconstructed volume of a representative fragment of 30CuZn-Z_M catalyst showing CuO particles sizes (a) 5.3 nm (pink circle) and (b) 2 nm (red arrow). (For interpretation of the references to colour in this figure legend, the reader is referred to the web version of the article.)

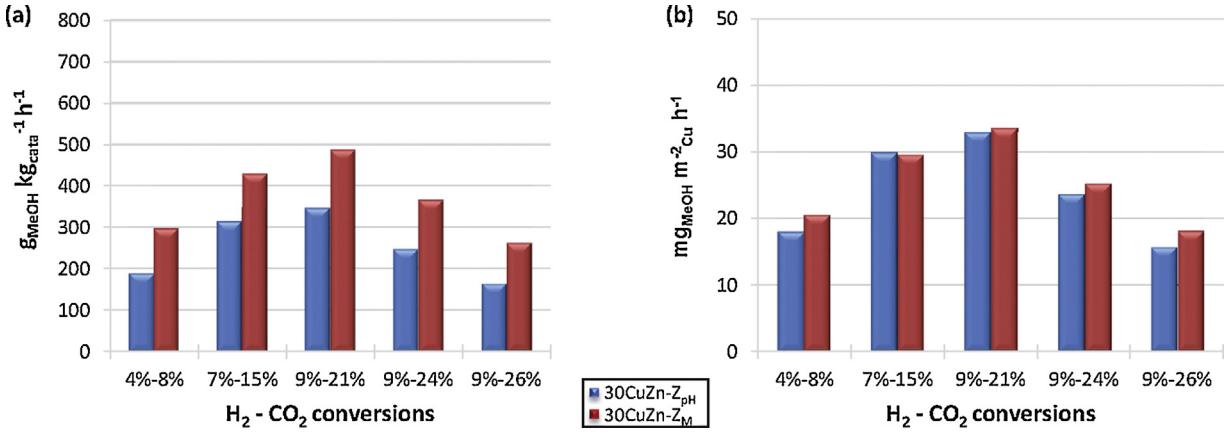

Fig. 10. Productivity of 30CuZn-Z_{pH} and 30CuZn-Z_M catalysts in CO_2 hydrogenation reaction at 50 bar and a GHSV of 10,000 h^{-1}.

Table 2
Catalytic results of 30CuZn-Z_{pH} and 30CuZn-Z_M catalysts in CO_2 hydrogenation reaction at 50 bar and a GHSV of 10,000 h^{-1}.

Catalyst	Catalyst mass (mg)	Reaction temperature (°C)	Conversion (%)		Selectivity (%)		MeOH productivity (g_{MeOH} kg_{cata}^{-1} h^{-1})
			H_2	CO_2	MeOH	CO	
30CuZn-Z_{pH}	125	240	7.2	13.7	50	50	314
		260	9.4	19.6	50	50	453
		280	10.0	22.2	34	66	346
		300	9.6	24.0	22	78	248
		320	9.1	25.7	14	86	165
30CuZn-Z_M	84	240	4.5	9.3	47	53	298
		260	7.1	15.1	42	58	429
		280	9.2	21.0	34	66	486
		300	9.0	23.9	22	78	366
		320	9.4	26.8	14	86	262

4. Conclusions

The effect of the synthesis method on the optimization of CuO-ZnO-ZrO_2 catalysts have been investigated and it was found that the continuous micro-fluidic coprecipitation provides a much more homogeneous and repeatable catalyst leading to better metallic copper surface area directly correlated to a better reactivity observed for the catalytic hydrogenation of carbon dioxide into methanol. The best methanol productivity was obtained for 30CuZn-Z_M catalyst with 486 g_{MeOH} kg_{cata}^{-1} h^{-1} at 280 °C under 50 bar and a GHSV of 10,000 h^{-1}, compared to 346 g_{MeOH} kg_{cata}^{-1} h^{-1} in the same conditions for the catalyst of identical composition prepared by batch coprecipitation.

This new synthesis method will therefore allow to control and vary different synthesis parameters (pH, temperature, molar ratio of carbonate/metal cations, speed flow, droplet size) in order to

Please cite this article in press as: L. Angelo, et al., Catalyst synthesis by continuous coprecipitation under micro-fluidic conditions: Application to the preparation of catalysts for methanol synthesis from CO_2/H_2, Catal. Today (2015), http://dx.doi.org/10.1016/j.cattod.2015.09.028

obtain better copper surface areas and Cu/ZnO/ZrO_2 interfaces to improve the Cu-ZnO-ZrO_2 systems reactivity.

Acknowledgements

The authors acknowledge the ANR for the financial support (project Vitesse^2 no. ANR-10-EESI-06).

References

[1] A. Goeppert, M. Czaun, J.P. Jones, G.K. Surya Prakash, G.A. Olah, Chem. Soc. Rev. 43 (2014) 7995–8048.
[2] G.A. Olah, G.K. Surya Prakash, A. Goeppert, J. Am. Chem. Soc. 133 (2011) 12881–12898.
[3] G.A. Olah, A. Goeppert, G.K. Surya Prakash, J. Org. Chem. 74 (2009) 487–498.
[4] J. Wambach, A. Baikerb, A. Wokaun, Phys. Chem. Chem. Phys. 1 (1999) 5071–5080.
[5] N.S. Shamsul, S.K. Kamarudin, N.a. Rahman, N.T. Kofli, Renew. Sust. Energ. Rev. 33 (2014) 578–588.
[6] C. Maldonado, J.G. Fierro, G. Birke, P. Martinez, J. Chil. Chem. Soc. 55 (2010) 506–510.
[7] F.J. Keil, Microporous Mesoporous Mater. 29 (1999) 49–66.
[8] M. Aresta, A. Dibenedetto, A. Angelini, J. CO_2 Util. 3–4 (2013) 65–73.
[9] J.E. Jackson, F.M. Bertsch, J. Am. Chem. Soc. 112 (1990) 9085–9092.
[10] M. Bjørgen, F. Joensen, M. Spangsberg Holm, U. Olsbye, K.-P. Lillerud, S. Svelle, Appl. Catal. A Gen. 345 (2008) 43–50.
[11] G.A. Olah, Angew. Chem. Int. Ed. Engl. 44 (2005) 2636–2639.
[12] L. Feng, W. Cai, C. Li, J. Zhang, C. Liu, W. Xing, Fuel 94 (2012) 401–408.
[13] S.D. Knights, K.M. Colbow, J. St-Pierre, D.P. Wilkinson, J. Power Sources 127 (2004) 127–134.
[14] E. Audibert, A. Raineau, Ind. Eng. Chem. 20 (1928) 1105–1110.
[15] Z.-X. Ren, J. Wang, L.-J. Jia, D.-S. Lu, Appl. Catal. 49 (1989) 83–90.
[16] J.S. Lee, K.H. Lee, S.Y. Lee, Y.G. Kim, J. Catal. 144 (1993) 414–424.
[17] Q. Sun, C. Liu, W. Pan, Q. Zhu, J. Deng, Appl. Catal. A Gen. 171 (1998) 301–308.
[18] T. Fujitani, J. Nakamura, Appl. Catal. A Gen. 191 (2000) 111–129.
[19] E.L. Kunkes, F. Studt, F. Abild-Pedersen, R. Schlögl, M. Behrens, J. Catal. 328 (2015) 43–48.
[20] F. Arena, K. Barbera, G. Italiano, G. Bonura, L. Spadaro, F. Frusteri, J. Catal. 249 (2007) 185–194.
[21] K. Kobl, L. Angelo, Y. Zimmermann, S. Sall, K. Parkhomenko, A.C. Roger, C.R. Chim. 18 (2015) 302–314.
[22] R. Zhou, T. Yu, X. Jiang, F. Chen, X. Zheng, Appl. Surf. Sci. 148 (1999) 263–270.
[23] R.A. Koeppel, A. Baiker, Appl. Catal. A Gen. 84 (1992) 77–102.
[24] L. Angelo, K. Kobl, L.M. Martinez Tejada, Y. Zimmermann, K. Parkhomenko, A.C. Roger, C.R. Chim. 18 (2015) 250–260.
[25] G. Prieto, K.P. De Jong, P.E. De Jongh, Catal. Today 215 (2013) 142–151.
[26] C. Kiener, M. Kurtz, H. Wilmer, C. Hoffmann, H.W. Schmidt, J.D. Grundwaldt, M. Mulher, F. Schüth, J. Catal. 216 (2003) 110–119.
[27] C. Baltes, S. Vukojevic, F. Schüth, J. Catal. 258 (2008) 334–344.
[28] M. Schur, B. Bems, A. Dassenoy, I. Kassatkine, J. Urban, H. Wilmes, O. Hinrichsen, M. Muhler, R. Schlögl, Angew. Chem. Int. Ed. Engl. 42 (2003) 3815–3817.
[29] X. Yao, Y. Zhang, L. Du, J. Liu, J. Yao, Renew. Sust. Energ. Rev. 47 (2015) 519–539.
[30] S. Kühl, M. Friedrich, M. Armbrüster, M. Behrens, J. Mater. Chem. 22 (2012) 9632–9638.
[31] H. Song, D.L. Chen, R.F. Ismagilov, Angew. Chem. Int. Ed. Engl. 45 (2006) 7336–7356.
[32] K.I. Sotowa, K. Irie, T. Fukumori, K. Kusakabe, S. Sugiyama, Chem. Eng. Technol. 30 (2007) 383–388.
[33] S.-Y. Teh, R. Lin, L.-H. Hung, A.P. Lee, Lab Chip 8 (2008) 198–220.
[34] P. Mierczynski, T.P. Maniecki, K. Chalupka, W. Maniukiewicz, W.K. Jozwiak, Catal. Today 176 (2011) 21–27.
[35] M. Behrens, D. Brennecke, F. Girgsdies, S. Kißner, A. Trunschke, N. Nasrudin, S. Zakaria, N.F. Idris, S.B.A. Hamid, B. Kniep, R. Fischer, W. Busser, M. Muhler, R. Schlögl, Appl. Catal. A Gen. 392 (2011) 93–102.
[36] C. Serra, N. Berton, M. Bouquey, L. Prat, G. Hadziioannou, Langmuir: ACS J. Surf. Colloids 23 (2007) 7745–7750.
[37] H.P. Kulg, L.E. Alexander, X-ray Diffraction Procedures, John Wiley and Sons, New York, 1954.
[38] G. Chinchen, C.M. Hay, H.D. Vandervell, K.C. Waugh, J. Catalysis 103 (1987) 79–86;
[X] K. Kobl, Aspects mécanistiques et cinétiques de la production catalytique de méthanol à partir de CO_2/H_2, Thèse de doctorat de l'Université de Strasbourg (2015).
[39] J.W.W. Evans, M.S.S. Wainwright, D.J. Young, A.J. Bridgewater, Appl. Catal. 7 (1983) 75–83.
[40] J.R. Kremer, D.N. Mastronarde, J.R. McIntosh, J. Struct. Biol. 116 (1996) 71–76.
[41] C. Messaoudi, T. Boudier, C.O.S. Sorzano, S. Marco, BMC Bioinf. 8 (2003) 288.
[42] H. Jeong, K.I. Kim, T.H. Kim, C.H. Ko, H.C. Park, I.K. Song, J. Power Sources 159 (2006) 1296–1299.
[43] F. Arena, R. Giovenco, T. Torre, A. Venuto, A. Parmaliana, Appl. Catal. B 45 (2003) 51–62.
[44] G. Bonura, F. Arena, G. Mezzatesta, C. Cannilla, L. Spadaro, F. Frusteri, Catal. Today 171 (2011) 251–256.
[45] G. Bonura, M. Cordaro, C. Cannilla, F. Arena, F. Frusteri, Appl. Catal. B 152–153 (2014) 152–161.
[46] M. Saito, T. Fujitani, M. Takeuchi, T. Watanabe, Appl. Catal. A Gen. 138 (1996) 311–318.

Please cite this article in press as: L. Angelo, et al., Catalyst synthesis by continuous coprecipitation under micro-fluidic conditions: Application to the preparation of catalysts for methanol synthesis from CO_2/H_2, Catal. Today (2015), http://dx.doi.org/10.1016/j.cattod.2015.09.028